Effect of borax on the wetting properties and crystallization behavior of sodium sulfate

Granneman, Sanne; Shahidzadeh, Noushine; Lubelli, Barbara; van Hees, Rob

DOI
10.1039/C6CE02163H

Publication date
2017

Document Version
Accepted author manuscript

Post print version of http://dx.doi.org/10.1039/C6CE02163H

CrystEngComm

Paper

Effect of borax on wetting properties and crystallization behavior of sodium sulfate

Received 00th January 20xx,
Accepted 00th January 20xx

DOI: 10.1039/x0xx00000x

www.rsc.org/crystengcomm

Sanne J. C. Granneman,*[a] Noushine Shahidzadeh,[b] Barbara Lubelli,[a,c] and Rob P.J. van Hees[a,c]

Borax has been identified as possible crystallization modifier for sodium sulfate. Understanding the effect of borax on factors influencing transport and crystallization kinetics of sodium sulfate helps to clarify how this modifier might limit crystallization damage. It has been observed that the addition of borax to sodium sulfate solutions has no influence on the wetting properties (contact angle on glass, surface tension,or evaporation rate) and therefore will not influence solution transport. Additionally, the influence of borax on the crystallization kinetics of sodium sulfate was studied under controlled environmental conditions. This was done in mixtures in glass micro capillaries, and sequentially in droplets on glass plates. Under the here studied precipitation conditions, the addition of borax has no influence on the supersaturation ratio at the onset of crystallization, but it significantly affects the crystallization pattern of anhydrous sodium sulfate crystals (thenardite). Using RAMAN spectroscopy, two different hydrates of borax were identified after precipitation depending on the initial concentration of the solution. Each hydrate has a different effect on the subsequent crystallization of sodium sulfate. The decahydrate polymorph of borax leads to the precipitation of hydrated sodium sulfate crystals (mirabilite) and the pentahydrate form favors the precipitation of the anhydrous sodium sulfate crystals (thenardite) with an altered crystal habit. Using X-ray diffraction, overdevelopment of the (111), (131), (222) and (153) faces of thenardite was identified. Additionally, the ratios between several peaks is reversed. These results confirm the deviation of the grown crystals of the equilibrium crystal shape of thenardite as observed with optical microscopy.

Introduction

The crystallization of salts in porous building materials is an undesired event that can lead to severe damage and eventually degradation of the material.[1] The problem is expected to increase in the future due to climatic changes.[2] Salts can originate from e.g., sea salt spray, air pollutants or ground water penetrating via capillary absorption.[3] When salts crystallize on the outside of the material they cause esthetical unpleasant, but harmless efflorescence. However, when they crystallize in the pores of the material, as crypto-florescence, they are very harmful. Salt is damaging only if in combination with water: water dissolves the salt and transports it through the porous network of the material.[4] The wettability of the solution and material and the evaporation rate influence the solution transport. The constant interplay between advection of ions to the surface versus diffusive redistribution determines the salt distribution in the material.[5,6]

Despite extensive research[7-12], there is yet no definitive understanding of the mechanism of salt damage. The most diffused theory to describe the damage process is the theory of crystallization pressure.[13,14] A confined crystal will exert a pressure on the pore wall which depends on the supersaturation level of solution in contact with the crystal and the confining wall. One of the most damaging salts found in buildings is sodium sulfate; its harmfulness is mainly due to its multiple hydrates with different solubilities. Under ambient conditions the growth of two stable sodium sulfate crystal phases can be observed: the anhydrous thenardite and the decahydrated mirabilite.[15,16] During both cooling and drying experiments a metastable heptahydrate phase has also been observed.[17,18] The destructive effect of sodium sulfate is usually attributed to rapid crystallization of mirabilite crystals following dissolution of anhydrous sodium sulfate. When the anhydrous crystals start to dissolve, the solution will become supersaturated with respect to the less soluble mirabilite.[19,20] These rapid expanding clusters of mirabilite create stresses which are in excess of the tensile strength of most building materials.[21] Besides, the damage development is related to the degree of pore filling by the salt crystals.[22]

Additionally, recent publications highlight the importance of non-classical nucleation behavior and that the level of supersaturation reached in solution has a clear effect on the pathway of nucleation.[23] Usually, the crystal polymorph with the lowest solubility is expected to crystallize first, however, several experimental results prove otherwise. This implies that thermodynamic equilibrium considerations cannot explain the dynamic process, and kinetics instead of thermodynamics

[a] Department of Architectural Engineering + Technology, Delft University of Technology, Delft, 2628 BL, The Netherlands. E-mail: S.J.C.Granneman@tudelft.nl
[b] Institute of Physics, University of Amsterdam, Amsterdam, 1098 XH, The Netherlands.
[c] TNO Technical Sciences, Delft, 2600 AA, The Netherlands.

dominates the process. The high interfacial free-energy barriers for the formation of hydrated sodium sulfate crystals inhibit their formation, resulting in highly supersaturated solutions, with respect to the hydrated phase, upon further evaporation.[24]

Among building materials, lime-based mortars are particularly susceptible to salt damage, due to their limited mechanical strength and their bi-modal pore size distribution, with both fine and coarse pores, facts which are favorable to the development of damage. The traditional approach to mitigate damage is to alter the material properties to make them more resistant to salt decay. Examples are the use of water-repellent additives to prevent the ingress of (salt containing) water or the substitution of the lime binder with cement, in order to increase the mechanical strength. However, these solutions usually are not satisfactory due to their poor compatibility with the existing materials.[3,25]

Alternatively, it has been suggested to influence the damaging process itself, by using crystallization modifiers.[26-28] Previous research suggests the possibility of mixing these crystallization modifiers in a mortar already during its preparation.[29] This would make possible to the modifier to be immediately activated when the salts and water enter the material. Modifiers which are to be mixed in mortar need to meet two prerequisites: first, they have to remain effective after undergoing the pH change during carbonation of a lime mortar (a fresh lime mortar has a pH of 13, and a carbonated one pH 9); second, they have to be effective at the whole pH range, because damaging salts may already enter or be present in the material before the end of the carbonation process. Possible mechanisms of modifiers which may help to reduce the damage are: (i) keeping salts dissolved in solution (inhibitors) allowing for transport to the surface during evaporation; (ii) promoting the crystallization of a specific crystal phase (promoters) at or near saturation; (iii) changing the shape of the growing crystals (habit modifiers).[30] Beneficial effects of habit modification can for instance be seen in the case of ferrocyanide modification of sodium chloride. Due to the presence of ferrocyanide, the shape of the crystals changes from cubic to dendritic. During drying, the salt solution will creep along the branches of the dendrites. The larger evaporation surface of the branched crystals enhances transport of the solution to the drying surface, leading to harmless efflorescence instead of harmful crypto-florescences (see for instance Gupta et al.[31]). Depending on concentration, a modifier may exhibit different behavior.[32]

Well-known modifiers for sodium sulfate are phosphonates[26,28,33] Although they are effective as modifiers, they are most unsuitable to be mixed in a mortar due to their pH sensitivity. Phosphonates can work either as inhibitor or promoter depending on the pH range , and are typically active to a pH of ~8.5. At pH levels higher than 8.5, as it occurs in a mortar, the salt crystal surface becomes increasingly negative and this will lead to repulsive electrostatic forces between the ionized phosphonate molecules and the sodium sulfate which will limit the modifier effect.[33] A possible alternative for the phosphonates is borax ($Na_2B_4O_7{\cdot}10H_2O$, disodium tetraborate decahydrate), which is known to promote the precipitation of mirabilite at or near saturation.[34] Preliminary research suggests that borax can be used in a mortar, as it does not affect for example the carbonation process.[35] The influence of borax on sodium sulfate crystallization from solution has been studied in previous research.[36,37] However, the influence of different concentrations of borax on the crystallization kinetics of sodium sulfate has not been investigated in detail yet.

In this paper the interaction of borax and sodium sulfate was studied systematically. We show through thorough study of the physicochemical properties of water and sodium sulfate solutions, that the addition of borax has no influence on the wetting properties, i.e., contact angle and surface tension. However, when the impact of borax on the supersaturation level and the kinetics of growth of sodium sulfate solutions additivated with borax was assessed in glass micro capillaries during evaporation, different mechanisms of growth were observed. The consecutive crystallization of droplets of borax and sodium sulfate was studied with optical microscopy and RAMAN spectroscopy. This revealed that depending on the starting concentration of borax solution, two different crystalline phases can precipitate which each have a different effect on the subsequent sodium sulfate crystallization.

Materials and methods

Salt solutions and substrates

Salt solutions were prepared by adding Milli-Q grade water to borax (sodium tetraborate decahydrate, puriss., Sigma Aldrich) and/or sodium sulfate (sodium sulfate anhydrous, Ph Eur, Sigma Aldrich) and stirring until a homogeneous solution was obtained. For sodium sulfate a 1 mol/kg concentration was chosen, such that at the start of the experiments the solution was unsaturated with respect to all crystal phases, at the experimental temperature range of 20-25°C. This ensured that crystallization would not begin during the measurement of the solution properties or during preparation of the crystallization experiments. Borax concentrations ranged between 0.001-0.102 mol/kg in water (borax solubility is 0.13 mol/kg at 20°C[38]) and between 0.01-0.102 mol/kg in mixtures with 1 mol/kg sodium sulfate.

Evaporative crystallization of sodium sulfate with and without borax was studied in two series of experiments. First, in mixtures in glass micro-capillaries, to simulate a single pore in a porous medium.[39] This experiment allowed for the determination of the supersaturation level at the onset of crystallization. Second, on glass slides, where sequential crystallization of borax and sodium sulfate allowed for the identification of the different crystallized phases. This simulates the situation where the modifier is already present (in crystalline state) before interaction with the salt. In both experiments the effect of borax addition on the kinetics of crystallization of sodium sulfate was studied.

In order to have a clean surface, the cylindrical glass capillaries with 100 micrometer diameter were cleaned with ethanol. The Corning glass slides were cleaned in an ultrasonic

Table 1. Details of the different experiments

	T/RH%	Substrate	Solutions [aq]
Surface tension	25.0°C ± 0.5 67 RH% ± 3[a]	-	Water 0.001, 0.005, 0.010, 0.051 and 0.102 mol/kg borax 1 mol/kg Na_2SO_4 1 mol/kg Na_2SO_4 + 0.010 mol/kg borax 1 mol/kg Na_2SO_4 + 0.051 mol/kg borax 1 mol/kg Na_2SO_4 + 0.102 mol/kg borax
Contact angle	25.0°C ± 0.5 67 RH% ± 3[a]	Corning glass slide	1 mol/kg Na_2SO_4 1 mol/kg Na_2SO_4 + 0.010 mol/kg borax 1 mol/kg Na_2SO_4 + 0.051 mol/kg borax
Capillary	23.1°C ± 0.5 65.7 RH% ± 1.8[a]	100 µm glass capillary	1 mol/kg Na_2SO_4 + 0.051 mol/kg borax
Droplet	20°C ± 0.2 65 RH% ± 1.4[b]	Corning glass slide	0.010, 0.051, 0.102 mol/kg borax 1 mol/kg Na_2SO_4

[a]The temperature and relative humidity were controlled as described in Shahidzadeh et al.[40]
[b]Experiments were done in a CTS walk-in climatic chamber.

bath for 3 times 10 minutes with acetone, ethanol and water, consecutively, and then left to dry at ambient conditions. All experiments were carried out at controlled environmental conditions, either using the set-up described by Shahidzadeh et al.[40], or in a walk-in climatic chamber (CTS). A rather high relative humidity was chosen in order to simulate values found in practice.[7] The details per experiment are summarized in Table 1.

Experimental procedures

The wetting properties of water and sodium sulfate additivated with different concentrations of borax were determined using a KRUSS apparatus (EasyDrop FM40Mk2). The surface tension was measured using the pendant drop method. This standard method is based on the balance, at the moment a droplet breaks off from a capillary of known size, between gravity and the restoring surface tension.[39] The obtained values for the surface tension are an average of 10 repetitions. The equilibrium static contact angle of 2 µL droplets deposited on glass slides, was determined using imaging analysis. The contact angle is dependent on the wettability of the substrate and the surface tension of the solution.[41] The obtained contact angle is an average of 6 or more repetitions. The evaporation and crystallization in capillaries was followed using optical microscopy (Leica DM IRB) and direct imaging with a digital microscope camera.[39] Following the menisci, and the related volume variation in time allowed for the determination of the supersaturation level at the onset of crystallization. This method was already used in previous experiments to determine the supersaturation of sodium sulfate.[40] Here, the experiment on pure sodium sulfate was replicated in order to have a reference. Then, the same experimental setup was used to determine the supersaturation for mixtures additivated with borax. Additionally, the possible effect of borax on growth kinetics of sodium sulfate was studied. The experiment was replicated 4 times for both solutions.

Sequential crystallization of borax and sodium sulfate was studied by evaporating droplets of 25 µL. First, droplets of borax were evaporated on glass slides. Then, sodium sulfate droplets were evaporated on the glass or on the previously crystallized borax layer. During evaporation, the slides were placed in a box with partially closed cover to reduce draught (average air speed in the box was 0.13 m/s, measured with Testo 435 sensor), which can influence the evaporation rate. The crystallized phases of borax and sodium sulfate were examined and identified using RAMAN spectroscopy. The crystallization pattern of sodium sulfate with and without borax was studied using optical microscopy (Zeiss Axioplan). The effect of borax on the habit of sodium sulfate crystals was additionally studied using X-ray diffraction (Bruker D8 Advance X-ray diffractometer in Debye-Scherrer geometry, with an XYZ sample stage. Cu-Kα X-rays were generated at 40 kV and 40 mA). The XRD pattern was recorded directly on the glass without any further sample preparation. Phase identification was performed using Bruker Eva 4.1 software and appropriate databases (ICDD PDF2 2011). Rietveld refinement on the sample was performed with Topas 5.0.

Results and discussion

Wetting properties

The characterization of the physicochemical properties of solutions is important to account for the crystallization by evaporation in droplets and capillaries. Generally, the addition of salt (ions) increases the surface tension of water. According to the Young-Laplace equation, the latter has direct consequence on the spreading properties of the solution. As the evaporation rate of droplets is proportional to the perimeter of the droplet, this directly affects the evaporation rate which can lead to the precipitation of different polymorphs and therefore change the crystallization pattern.[41-43]

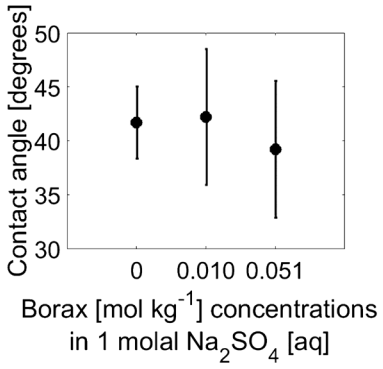

Figure 1. Contact angle on Corning glass slides of 2 µL droplets of 1 mol/kg sodium sulfate solution additivated with different concentrations of borax. Each point is an average of 6 or more repetitions.

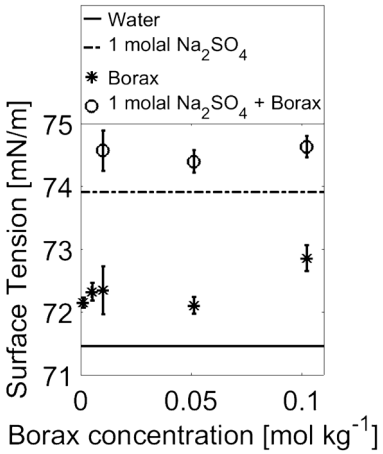

Figure 2. Surface tension values of borax in water or mixed with 1 mol/kg sodium sulfate in comparison to pure water and a 1 mol/kg sodium sulfate solution. Each point is an average of 10 measurements.

The measurements of contact angle and surface tension of water and sodium sulfate additivated with different concentrations of borax are depicted in Figures 1 and 2. The addition of borax has no distinct influence on the contact angle of sodium sulfate solution at any of the studied borax concentrations. In Figure 2 the horizontal lines represent the measured surface tension of pure water (71.5 mN/m) used to prepare the salt solutions and the measured surface tension of pure sodium sulfate solution at 1 mol/kg (73.9 mN/m). These values are in good agreement with those reported in the literature.[44] Upon addition of borax to water or sodium sulfate, there is only a slight increase of surface tension. These results show that the addition of small amounts of borax does not affect the physicochemical properties of the solution and therefore the results reported here on the crystallization of sodium sulfate in the presence of borax are not due to a confinement effect at the contact line of the droplet experiments, i.e., a change in evaporation rate and contact angle.[41] Additionally, since no spreading of the droplets is observed, no effect on the dynamics of solution transport is expected.

Crystallization in capillaries

Figures 3 and 4 show the precipitation and growth of the crystals within the first 300 seconds of the crystallization sequence in the capillaries. In Figure 3a it can be seen that, initially, phase(III) anhydrous sodium sulfate needles grow, which immediately dissolve again to form the more stable phase V prisms (Figure 3c). This sequence was also clearly observed in previous research.[40] In the case of the mixture with borax (Figure 4) crystallization of mirabilite was expected due to the promoter effect of borax reported in literature.[36] Instead, growth of anhydrous crystals occurred (for a borax concentration of 0.051 mol/kg). The absence of a hydrate was confirmed by placing the capillary in an oven at 70°C for 3 hours, and photographing the capillary before and after. No dehydration of the crystals was observed. Interestingly, in the presence of borax, the anhydrous sodium sulfate needles and prisms do not grow sequentially, but seem to grow simultaneously from the start. Then needle crystals dissolve

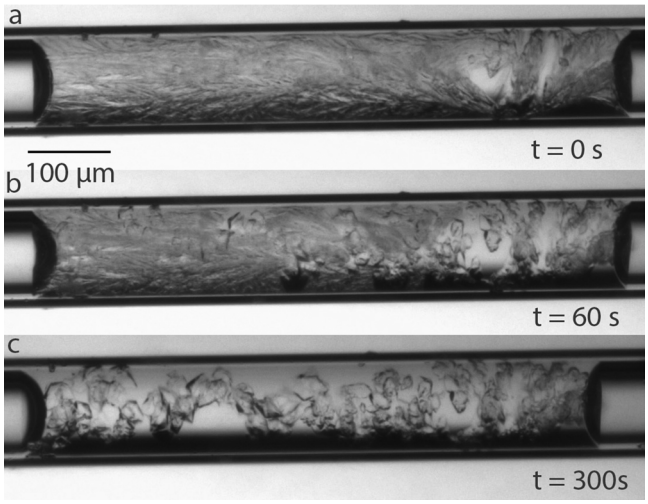

Figure 3. Crystallization of 1 mol/kg sodium sulfate solution in a glass capillary at the start (a) and after 60 s (b) and 300 s (c). Initially (a) anhydrous phase III needles form, which immediately dissolve to form the stable phase V prisms (c).

Figure 4. Crystallization of 1 mol/kg sodium sulfate solution mixed with 0.051 mol/kg borax in a glass capillary at the start (a) and after 65 (s) and 270 s (c). Both phase III and phase V anhydrous crystals form simultaneously (a). At the end of the shown sequence (c), all needles (phase III) have dissolved. The crystal habit of phase V is altered with respect to that observed in the absence of borax (compare to Figure 3c).

and at the end of the shown crystallization sequence, only prisms remain (Figure 4c), similar to the crystallization sequence without borax (Figure 3c). However, when Figures 3c and 4c are compared, it is clear that at the used concentration, the addition of borax leads to an alteration of the habit of anhydrous sodium sulfate crystals.

All the evaporation experiments are done in a climatic chamber at RH 65% which is a relative humidity representative of situations found in the field (in indoor situations). Moreover, the initial evaporation rate at this fixed RH decreases even more with time during the experiments in micro-capillaries. This can be clearly seen from the nonlinear behavior of the volume change in the micro-capillaries over time (Figure 5). In the micro-capillaries the evaporation rate is limited by diffusive vapor transport through the gas phase[45], following:

$$e = \rho_g D \frac{(c_i - c_\infty)}{\delta}$$

with ρ_g the vapor density, D the diffusion coefficient of water vapor through the gas, c_i and c_∞ are respectively the equilibrium relative humidity above the menisci and the relative humidity fixed in the climatic chamber (65%) and δ is the distance between the meniscus and the exit of the capillary. As it is clear from this equation, the evaporation rate slows down in our experiments firstly because the saturated vapour concentration above the menisci decreases when the salt solution becomes more concentrated and secondly because δ increases in time.

The slow evaporation during the experiment leads to a very homogeneous solution. As was shown in Desarnaud et al.[45], the nucleation rate is only dependent on the supersaturation, and is negligible below the limit of supersolubility. If local concentration fluctuations would occur, reaching the supersolubility limit, crystallization would start there and consume the supersaturation. The absence of concentration fluctuations limits the possibility of local nucleation and explains why high supersaturation ratios in the whole solution can be reached.

The evaporation rate of the solution was determined by following the distance between the two menisci of the liquid in the capillary in time. As already expected on the basis of the measured solution properties, no effect on evaporation rate due to addition of borax was observed. The distance between the menisci and the related volume was used for the determination of the supersaturation at the start of crystallization. m_0 is the initial concentration in solution (1 mol/kg) and m is the calculated concentration at the onset of crystallization. m_s is the saturation concentration of sodium sulfate phase III (4.4 mol/kg at the experimental condition of 23°C). The supersaturation S of the solution can then be determined using:

$$S = \frac{m}{m_s}$$

The following S values were found: in the case of sodium sulfate S= 1.25 ± 0.13, and for sodium sulfate with borax S= 1.22 ± 0.28.

When expressed in molar values, these values correspond to S= 1.14 ± 0.2 and S= 1.13 ± 0.06, respectively, values which are in good agreement with those reported in Shahidzadeh and Desarnaud.[40] The change in volume of the solution in the capillaries and the corresponding increase in concentration are plotted in Figure 5 (open markers correspond to sodium sulfate, closed markers to sodium sulfate + borax). The starting concentration (diamond) and the concentrations at the onset of crystallization (circle is sodium sulfate, square is sodium sulfate + borax) are indicated in the phase diagram in Figure 6. The phase diagram clearly shows that in both cases the solution is heavily supersaturated with respect to mirabilite (S is 3.68 and 3.64, respectively); however, no crystallization of this phase occurred. This supports the statement that highly supersaturated solutions can be formed resulting in crystallization of the more soluble anhydrous phase instead of less soluble hydrated crystals.

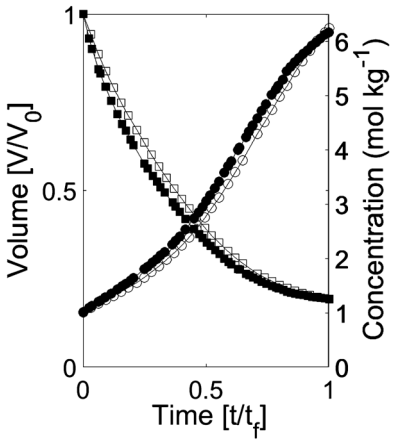

Figure 5. Normalized volume change and corresponding increasing concentration during evaporation of solution in capillaries till precipitation. Squares correspond to volume and circles to concentration. Open markers correspond to sodium sulfate, closed markers to sodium sulfate + borax.

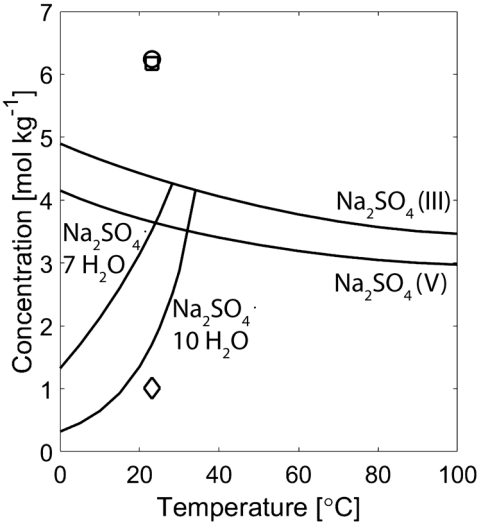

Figure 6. Phase diagram using the model from Steiger and Asmussen.[16] The diamond corresponds to the starting concentration in the capillary experiments. The circle (sodium sulfate) and square (sodium sulfate + borax) correspond to an average concentration at the onset of crystallization of 4 replicas.

Crystallization of droplets

The products of sequential evaporation of droplets of borax and then sodium sulfate on glass slides were studied using RAMAN spectroscopy (Renishaw InVia Raman spectrophotometer, 532nm laser). The position of the most abundant peak is given in Table 2 and the different salt phases were identified using literature spectra.

Crystallization of the different borax solutions resulted in two different phases of sodium tetraborate, depending on the starting concentration of solution. In the case of the highest concentration (0.102 mol/kg), sodium tetraborate decahydrate (borax) was formed. This concentration is close to the solubility of borax (0.13 mol/kg at 20°C[38]). This could mean that small crystallites of borax were still present in the solution, which then acted as seed crystals for further growth of borax upon evaporation of solution. Differently, for lower concentrations (0.010 and 0.051 mol/kg) sodium tetraborate pentahydrate (tincalconite) crystals were formed. Although it is known that, at the used environmental conditions, tincalconite and borax could convert to one another[46], it is not known how and if this behavior can be related to the starting concentration of the borax solution.

Figure 7 shows different crystallized droplets of sodium sulfate. Figure 7A shows sodium sulfate crystals grown from a pure solution. These crystals were identified as the anhydrous phase V (thenardite). Sodium sulfate crystals grown on top of the tetraborate layers resulted in different sodium sulfate phases depending on the type of tetraborate phase. In the case of borax, hydrated crystals of sodium sulfate were formed (Figure 7B), which immediately dehydrated, leaving the characteristic opaque/white crystals, previously identified as the dehydration product.[15] This hydrate is most likely mirabilite, due to its lattice similarity with borax.[36] The hydrated crystals could not be identified using RAMAN, because it was not possible to control temperature and relative humidity in the used set-up during measurements. Therefore, as soon as the hydrated crystals were placed in the RAMAN, they started to dehydrate, resulting in the

Table 2. Identification of crystal phases measured from evaporative crystallization from droplets, using RAMAN spectroscopy.

Compound	Peak position (cm-1) Measured (± 0.9)	Literature (phase)
Borax 0.010 mol/kg	577.7	577.20 (tincalconite)[a]
Borax 0.051 mol/kg	577.7	577.20 (tincalconite)[a]
Borax 0.102 mol/kg	574.0	573.96 (borax)[a]
Na_2SO_4 (pure)	991.7	993.20 (thenardite)[b]
Na_2SO_4 (on 0.051 mol/kg borate)	991.7	993.20 (thenardite)[b]
Na_2SO_4 (mix with 0.051 mol/kg borate)	992.6	993.20 (thenardite)[b]

[a]Phase identification according to Lafuente et al.[47]
[b]Phase identification according to Linnow et al.[48]

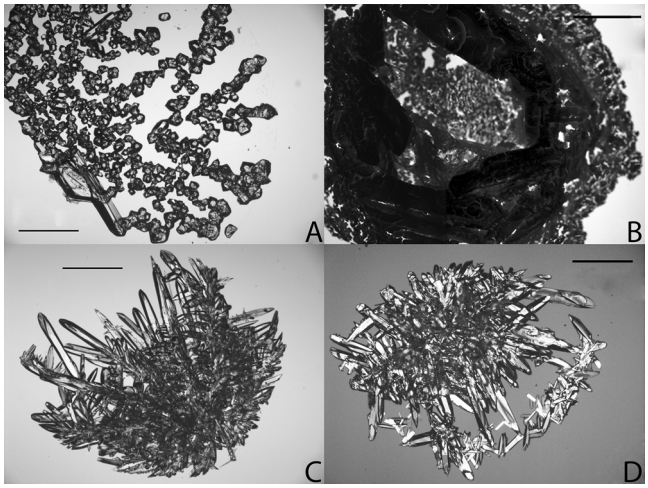

Figure 7. A: Sodium sulfate crystals without tetraborate, displaying the characteristic prisms of anhydrous thenardite. B: Dehydrated sodium sulfate crystals (mirabilite) grown on top of sodium tetraborate decahydrate (borax). C: Thenardite crystals precipitated by evaporation of sodium sulfate on top of sodium tetraborate pentahydrate (tincalconite). D: Thenardite crystals grown from a mixture of 0.051 mol/kg borax and 1 mol/kg sodium sulfate. Scale bars: 500 μm.

measurement of thenardite. Figure 7C shows crystals of sodium sulfate grown on top of a previous layer of tincalconite. These crystals gave the same signal as the ones without borax, and were thus also identified as the anhydrous sodium sulfate phase V (thenardite). However, the crystals show a clearly altered crystallization habit compared to the anhydrous sodium sulfate crystals grown without borax, which display the equilibrium crystal shape. Figure 7D shows sodium sulfate crystals grown from a mixture of sodium sulfate and 0.051 mol/kg borax. These crystals were identified as anhydrous sodium sulfate phase V crystals (thenardite) as well.

When comparing sodium sulfate grown in the presence of 0.051 mol/kg tetraborate, either mixed in solution (Figure 4 or Figure 7D) or in crystalline phase (Figure 7C), a similarity in crystal habit can be observed. Apparently, for the tetraborate to be effective as a habit modifier, it is enough that it is present in solution, not necessarily in the crystalline state. During the evaporation experiment in the capillaries, the set-up was continuously monitored and no crystals other than needles or needles/prisms combined (thenardite) were observed. We cannot completely exclude that very small crystallites of a borax phase, not detectable with the used technique, might be present in solution prior to thenardite crystallization. It is important to note that both the capillary and the droplet experiments deal with a first event of crystallization. The effect of tetraborate on repeated dissolution/crystallization cycles is unknown yet and will be the object of future research.

In addition to visual inspection of the crystals with optical microscopy, the thenardite crystals from Figure 7C were examined using X-ray diffraction. This method was applied as an indirect way to observe preferential orientation of the crystals in order to further study the habit change and determine which faces are overdeveloped. In Figure 8, the measured pattern is compared to the literature pattern in order to assign indices to the peaks. The peaks at 25.9 and

39.9 2Theta values belong to the (3 -1 -2) and (4 -1 5) planes of the underlying tincalconite, respectively, and were therefore not indexed. Peak splitting in the measured pattern is due to the fact that Cu X-rays are generated at two different wavelengths: Cu-Kalpha1: 1.54056 Angstrom and Cu-Kalpha2: 1.54439 Angstrom. This effect becomes more pronounced at higher 2Theta values. The literature pattern is predicted using only Cu-Kalpha1=1.54056 Angstrom. To determine relative counts, the value of the 113 peak in the predicted pattern was set to 1. The measured pattern shows that there is an overdevelopment of the (111), (131), (222) and (153) faces of thenardite. Additionally, the ratios between several peaks, e.g. 111/113, 111/222 and 222/220, is reversed. These results confirm the deviation of the grown crystals of the equilibrium crystal shape of thenardite as was already observed with optical microscopy. Summarizing, it can be stated that, at the used concentration in this study, borax acts as a habit modifier of thenardite.

In Figure 9 the equilibrium morphology of thenardite and an altered morphology in the presence of sodium tetraborate are visualized. To model the altered morphology of thenardite, the distance to the centre of the crystal of the (153) face was decreased, considering that this peak showed the largest alteration in the measured XRD pattern. As can be seen in Figure 9E and F, the shape of the altered crystal displays more of a needle shape than prismatic as seen in the equilibrium crystal. Although tincalconite and thenardite are found together in nature (see e.g. Pabst and Sawyer, 1948[49]), to our knowledge, in literature there is no mention about a possible interaction mechanism between them. It is clear that the presence of tetraborate has a kinetic effect on the crystallization process, altering the growth of the crystal faces.[50] Considering that {153} is the dominant form of the altered thenardite crystals in the presence of tetraborate, this could indicate that the tetraborate ions incorporate on active sites on this crystal face. Tetraborate ions would hinder the growth of this crystal face, making it become more important for the final morphology of the grown crystals. A similar mechanism was already observed for the interaction between borax and epsomite.[36] If and how tetraborate adsorbs on thenardite might be determined using computer simulations (see e.g., Jiang et al.[32]). However, this is beyond the scope of the current research.

Figure 8. Top: Measured XRD pattern of crystals shown in Figure 7C. The crystals were identified as thenardite, according to PDF 01-07402936. Bottom: Pattern from PDF 01-07402936 used for peak assignation. The measured pattern shows an overdevelopment of the {153} face.

Conclusions

Contact angle, surface tension and evaporation rate of sodium sulfate solutions additivated with different borax concentrations were measured. The results showed that borax addition has no impact on these factors which influence wetting and solution transport. Additionally, two types of experiments were done to study crystallization kinetics and crystallization pattern of sodium sulfate. First, the evaporation of sodium sulfate solutions without and of solutions additivated with borax was studied in capillaries. The volume change and the associated concentration increase were determined, which allowed for the calculation of the supersaturation ratio at the onset of crystallization. Solutions without and solutions additivated with borax both resulted in anhydrous sodium sulfate crystals, at similar levels of supersaturation. This indicates that in our system there is no inhibitor or promoter effect of borax at the used concentrations. However, a clear alteration in crystal habit of the sodium sulfate crystals was observed in the presence of borax. Second, in order to identify the different crystallizing phases, crystallization of borax and sodium sulfate was studied in sequence in droplets. Evaporation of borax solutions under controlled environmental conditions resulted in the crystallization of two different sodium tetraborate hydrates depending on the starting concentration of borax: a starting concentration of 0.102 mol/kg results in the decahydrate (borax), whereas a starting concentration of 0.010/0.051 mol/kg results in the pentahydrate (tincalconite).

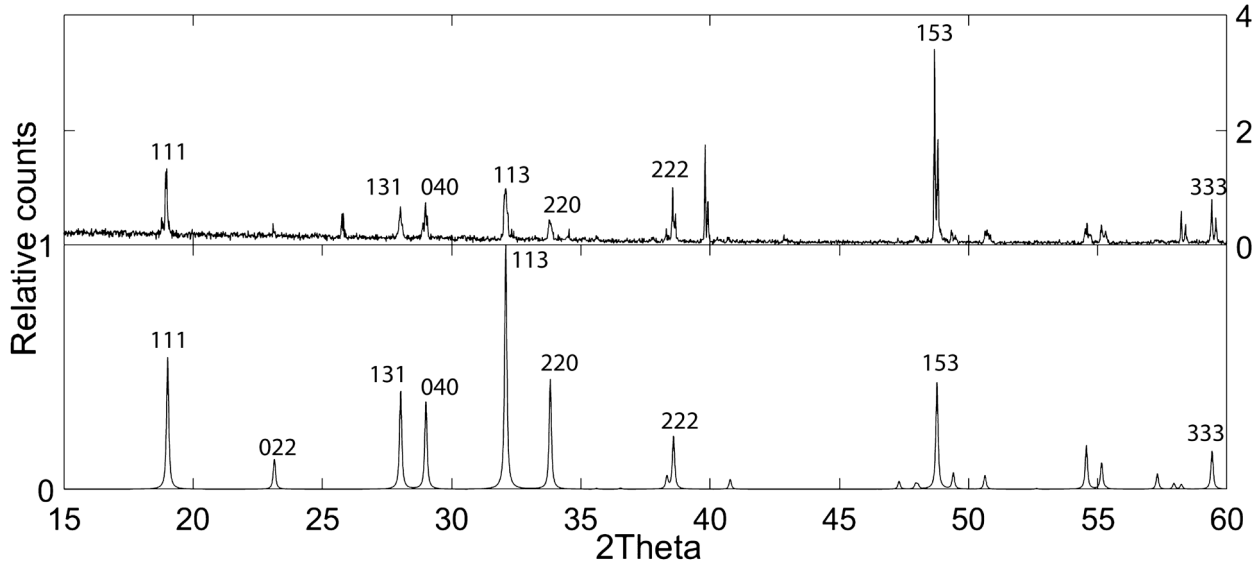

Sodium sulfate crystallization on top of borax resulted in crystallization of hydrated sodium sulfate crystals (mirabilite), whereas crystallization of sodium sulfate on top of tincalconite resulted in anhydrous sodium sulfate crystals (thenardite). Apparently, mirabilite is only grown in the presence of borax crystals, and not with tincalconite, as a consequence of the similarity in crystal lattice structure. The thenardite crystals grown in the presence of tincalconite showed an altered crystallization pattern compared to thenardite crystals displaying the equilibrium crystal shape grown from a pure solution. The altered crystal habit in the droplets resembled the altered habit seen in the capillaries. Using X-ray diffraction, it was identified that the altered crystal habit is due to an overdevelopment of the (111), (131), (222) and (153) faces and a reversal of the intensity ratios between several of these peaks. These results confirm the deviation of the grown crystals of the equilibrium crystal shape of thenardite as observed with optical microscopy.

Acknowledgements

The authors would like to thank Johan Bijleveld with his help on the measurement of the RAMAN spectroscopy. The authors also wish to thank Willem Duvalois, Timo Nijland and Rene de Gelder for their help with the measurement and analysis of the X-ray diffraction pattern. Finally, we would like to acknowledge the Dutch IOP program on Self-Healing Materials for funding (Grant number SHM012018).

Figure 9. Crystal structures drawn using the software VESTA.51 Top A-C: Equilibrium shape of thenardite using lattice parameters of PDF 01-07402936, visualized along a, b or c axis respectively. Bottom D-F: Schematic of the overdeveloped {153} crystal shape of thenardite as observed in the presence of sodium tetraborate, visualized along the a, b or c axis respectively.

References

1 A. Goudie and H. Viles, Salt weathering hazards, John Wiley & Sons, 1997.
2 T. G. Nijland, O. C. G. Adan, R. P. J. van Hees and B. D. van Etten, Heron, 2009, 54, 37–48.
3 A. Arnold, in Origin, mechanisms and effects of salts on degradation of monuments in marine and continental environments. Protection and Conservation of European Cultural Heritage., ed. F. Zezza, Bari, 1994, ch. Origin and behaviour of some salts in the context of weathering on monuments.
4 A. E. Charola and E. Wendler, Restoration of buildings and monuments, 2015, 21, 55–65.
5 L. Pel, H. Huinink and K. Kopinga, Applied Physics Letters, 2002, 81, 2893–2895.
6 J. Petkovic, H. P. Huinink, L. Pel, K. Kopinga and R. P. J. van Hees, Construction and Building Materials, 2010, 24, 118–127.
7 A. Arnold and K. Zehnder, The conservation of monuments in the Mediterranean Basin: the influence of coastal environment and salt spray on limestone and marble. Proceedings of the 1st International Symposium, Bari, 7-10 June 1989.
8 C. Rodriguez-Navarro and E. Doehne, Earth surface processes and landforms, 1999, 24, 191–209.
9 A. E. Charola, Journal of the American Institute for Conservation, 2000, 39, 327–343.
10 E. Doehne, in Natural stone, weathering phenomena, conservation strategies and case studies, ed. S. Siegesmund, T. Weiss and A. Vollbrecht, The Geological Society of London, 2002, ch. Salt weathering: a selective review, pp. 51–64.
11 G. W. Scherer, Cement and concrete research, 2004, 34, 1613–1624.
12 R. M. Espinosa-Marzal and G. W. Scherer, Accounts of chemical research, 2010, 43, 897–905.
13 C. W. Correns, Discussions of the Faraday Society, 1949, 5, 267–271.

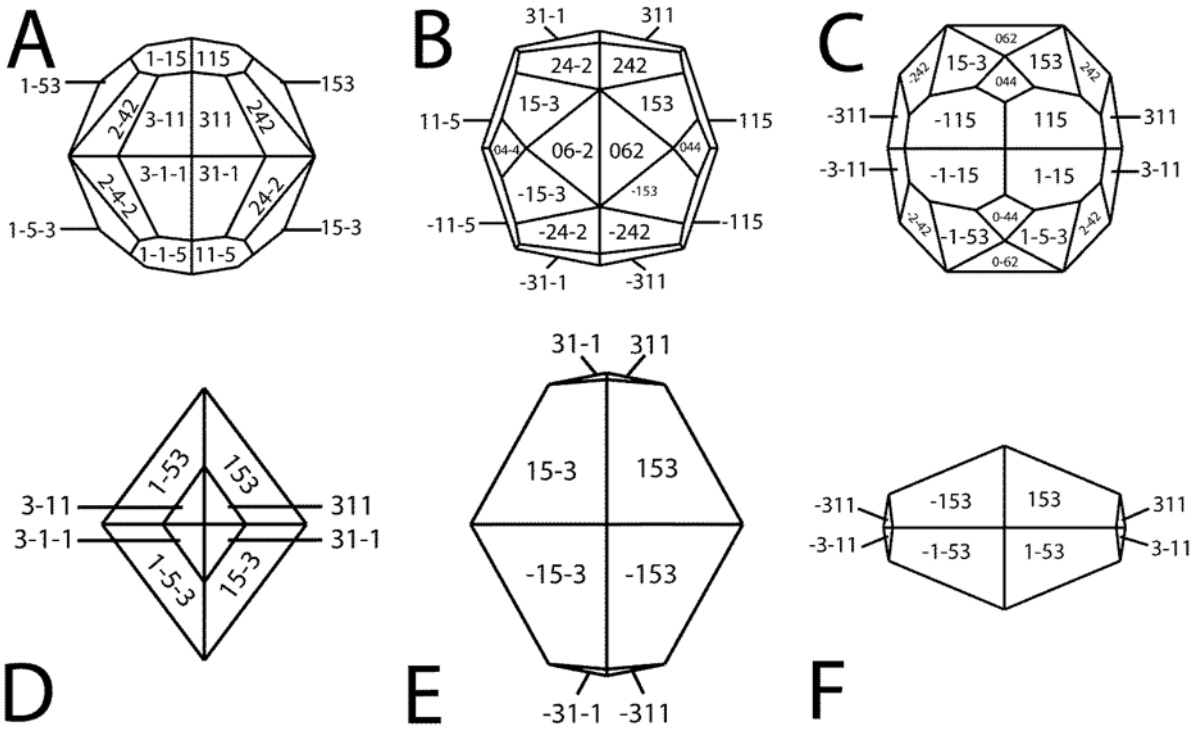

14 M. Steiger, Journal of Crystal Growth, 2005, 282, 455–469.
15 C. Rodriguez-Navarro, E. Doehne and E. Sebastian, Cement and concrete research, 2000, 30, 1527–1534.
16 M. Steiger and S. Asmussen, Geochimica et Cosmochimica Acta, 2008, 72, 4291–4306.
17 A. Hamilton and C. Hall, Journal of Analytical Atomic Spectrometry, 2008, 23, 840–844.
18 T. A. Saidov, L. Pel and G. H. A. van der Heijden, International Journal of Heat and Mass Transfer, 2015, 83, 621–628.
19 R. J. Flatt, Journal of Crystal Growth, 2002, 242, 435–454
20 J. Desarnaud, F. Bertrand and N.Shahidzadeh-Bonn, Journal of Applied Mechanics, 2013, 80, 020911-1-020911-7
21 N. Shahidzadeh-Bonn, J. Desarnaud, F. Bertrand, X. Chateau, X. and D. Bonn, Physical Review E, 2010, 81
22 R. J. Flatt, F. Caruso, A.M. Aguilar Sanchez and G.W. Scherer, Nature Communications, 2014, 5, 4823
23 S. Lee, H.S. Wi; W. Jo, Y.C. Cho, H. H. Lee, S.-Y. Jeong, Y.-I. Kim and G.W. Lee, PNAS, 2016, 113, 13618-13623
24 D. Bonn and N. Shahidzadeh, PNAS, 2016, *113*, 13551–13553
25 R. P. J. van Hees, S. Naldini and J. Delgado Rodrigues, Construction and Building Materials, 2009, 23, 1714–1718.
26 C. Selwitz and E. Doehne, Journal of Cultural Heritage, 2002, 3, 205–216.
27 B. Lubelli and R. P. J. van Hees, Journal of Cultural Heritage, 2007, 8, 223–234.
28 C. Rodriguez-Navarro and L. G. Benning, Elements, 2013, 9, 203–209.
29 B. Lubelli, T. G. Nijland, R. P. J. van Hees and A. Hacquebord, Construction and Building Materials, 2010, 24, 2466–2472.
30 F. Jones and M. I. Ogden, CrystEngComm, 2010, 12, 1016–1023.
31 S. Gupta, K. Terheiden, L. Pel, and A. Sawdy, Crystal Growth & Design, 2012, 12, 3888-3898
32 W. Jiang, H. Pan, J. Tao, X. Xu and R. Tang, Langmuir, 2007, 23, 5070–5076.
33 E. Ruiz-Agudo, C. Rodriguez-Navarro and E. Sebastián-Pardo, Crystal Growth & Design, 2006, 6, 1575–1583.
34 M. Telkes, Industrial and Engineering Chemistry, 1952, 44, 1308–1310.
35 S. J. C. Granneman, E. Ruiz-Agudo, B. Lubelli, R. P. J. van Hees and C. Rodriguez-Navarro, Proceedings of the 1st International Conference on Ageing of Materials and Structures, 2014.
36 E. Ruiz-Agudo and C. Rodriguez-Navarro, in Limestone in the built environment: present-day challenges for the preservation of the past, Geological Society, London, Special Publications, 2010, ch. Suppression of salt weathering of porous limestone by borax-induced promotion of sodium and magnesium sulphate crystallization, pp. 93–102.
37 M. Schiro, E. Ruiz-Agudo, and C.Rodriguez-Navarro, Physical Review Letters, 2012, 109
38 A. Apelblat and E. Manzurola, Journal of Chemical Thermodynamics, 2003, 35, 221–238.
39 N. Shahidzadeh-Bonn, S. Rafaï, D. Bonn and G. Wegdam, Langmuir, 2008, 24, 8599–8605.
40 N. Shahidzadeh and J. Desarnaud, The European physical journal applied physics, 2012, 60.
41 N. Shahidzadeh, M. F. L. Schut, J. Desarnaud, M. Prat and D. Bonn, Scientific Reports, 2015, 5, 10335.
42 N. Shahidzadeh-Bonn, S. Rafaï, A. Azouni, and D. Bonn, Journal of fluid mechanics, 2006, 549, 307-313
43 T.A. Saidov, N. Shahidzadeh, and L. Pel, *EPL,* 2013, 102, 28003
44 J. Desarnaud and N. Shahidzadeh-Bonn, EPL, 2011, 95.
45 J. Desarnaud, H. Derluyn, J. Carmeliet, D. Bonn, and N. Shahidzadeh, The journal of Physical Chemistry Letters, 2014, 5, 890-895
46 C. L. Christ and R. M. Garrels, American Journal of Science, 1959, 257, 516–528.
47 B. Lafuente, R. Downs, H. Yang and N. Stone, in Highlights in mineralogical crystallography, ed. T. Armbruster and R. M. Danisi, W. De Gruyter, 2015, ch. The power of databases: the RRUFF project, pp. 1–30.
48 K. Linnow, M. Steiger, C. Lemster, H. de Clercq and M. Jovanović, Environmental Earth Sciences, 2013, 69, 1609–1620.
49 A. Pabst, and D. L. Sawyer, American Mineralogist, 1948, 33, 472-481
50 S. Al-Jibbouri, C. Strege and J. Ulrich, Journal of Crystal Growth, 2002, 236, 400-406
51 K. Momma, and F. Izumi, Journal of Applied Crystallography, 2011, 44, 1272-1276